SEMARAK ILMU PUBLISHING

Journal of Advanced Research in Fluid Mechanics and Thermal Sciences

Journal homepage:
https://semarakilmu.com.my/journals/index.php/fluid_mechanics_thermal_sciences/index
ISSN: 2289-7879

Pico Scale Turgo Turbine Design for Remote Areas Application Using Velocity Triangle Approach

Imam Syofii[1], Andre Brilian Hidayatullah[2], Dendy Adanta[2,*], Dewi Puspita Sari[1], Firmansyah Burlian[2], Muhammad Amsal Ade Saputra[2]

[1] Study Program of Mechanical Engineering Education, Faculty of Teacher Training and Education, Universitas Sriwijaya, Ogan Ilir – 30662, South Sumatera, Indonesia
[2] Department of Mechanical Engineering, Faculty of Engineering, Universitas Sriwijaya, Ogan Ilir – 30662, South Sumatera, Indonesia

ARTICLE INFO

Article history:
Received 22 March 2022
Received in revised form 26 May 2022
Accepted 6 June 2022
Available online 1 July 2022

Keywords:
Turgo turbine; pico hydro; velocity triangle; remote areas; renewable energy

ABSTRACT

The global warming issue drives pico-scale hydropower plants to become the leading research focus. Pico-scale Turgo turbine (PSTT) is a suitable proposal to be developed as a power plant because it is cheap, easy to manufacture, and simple in shape and design. Although PSTT has been developed for a long time, the final decision on the optimum parameters of the jet angle and the blade angle does not exist, and the precision manufacturing technology for PSTT blade manufacturing has not received special attention. Hence, this study aims to evaluate the jet angle and the geometry of the pico-scale Turgo turbine spoon using velocity triangle analysis. The design of the blades is manufactured using a three-dimensional (3D) printing machine for performance tests. Based on comparing experimental results to analytical data, the velocity triangle approach is recommended for designing PSTT because of the average deviation of 6.6%. The deviation is considered reasonable. Then, based on calculations, the peak PSTT performance is predicted to occur at 20° the jet angle. This hypothesis is similar to previous studies; this indicates that the mathematical analysis using velocity triangle analysis is verified and recommended to be used.

1. Introduction

To increase the electrification ratio in Indonesia, new renewable energy is prospective to be utilized since Indonesia's water-energy potential reaches 19 GW for low scale and 75 GW for large scale. Converting water energy into electrical energy needs to be a particular concern [1]. The Turgo turbine is a suitable choice for converting pico-scale water energy (<5 kW) because of its simple design and construction and low investment costs [2]. Hence, pico-scale Turgo turbines (PSTT) are recommended as the independent power plant in remote areas of Indonesia [3-5]. Furthermore, the results of the Papua Terang Expedition (*Ekspedisi Papua Terang*) conducted by Limited Liability State Electricity Company of Indonesia (PT. PLN Indonesia) recommend using renewable energy based on

* *Corresponding author.*
E-mail address: dendyadanta@ymail.com

https://doi.org/10.37934/arfmts.97.1.157167

off-grid systems in remote areas. [6]. Pico hydro turbines (<5 kW) are the right solution to solve the problem of power generation in remote areas [7].

The Turgo turbine was invented and patented in 1920 by Gilkes Ltd. [8]. Turgo turbines are similar to Pelton's, but Turgo turbines have a jet attack angle as significant as 15 to 25°; water goes to the runner on one side, and out on the other. Therefore, the flow rate is not limited by the discharged water interfering with the incoming jet (as with Pelton turbines). Consequently, Turgo turbines have a smaller diameter than Pelton [9]. Turgo turbines convert the jet's water kinetic energy by the blade at atmospheric pressure. Turgo turbines are suitable for medium heads (H) between 10 to 50 m with discharge (Q) from 0.1 to 10 m^3/s [2].

The feasibility of a PSTT as independent power generation in remote or rural areas continues. Williamson *et al.,* [10] investigated the effect of the jet impact on PSTT performance using a two-dimensional quasi-steady-state model and validated it with experimental data. Based on the results, the jet impact position affects PSTT performance, and the middle location is recommended to be implemented [10]. Then, Gaiser *et al.,* [11] designed the PSTT blade using the response surface methodology (RSM); 4 parameters were quantified for their effect on performance (η): blade number (z), jet angle (α_1), nozzle diameter (d), and speed ratio (ϕ). Based on the results, four parameters identified significantly influence the performance of the PSTT [11]. Table 1 shows the geometry of Williamson *et al.,* [10] and Gaiser *et al.,* [11].

Table 1
Geometry and performance of studies by Williamson *et al.,* [10] and Gaiser *et al.,* [11]

Authors	α_1 (°)	β_1 (°)	β_2 (°)	ξ (°)	P_{mech} (W)	η (%)
Gaiser *et al.,* [11]	30	79	19	11	83	90
Williamson *et al.,* [10]	20	60	30	20	89.69	91

where β is blade angle, ξ is curvature angle, 1 is inlet position, and 2 is the outlet.

Table 1 shows that the geometry of Gaiser *et al.,* [11] has a mechanical power (P_{mech}) of 83 W with 90% efficiency, and Williamson *et al.,* [10] has a P_{mech} of 89.69 W and 91% efficiency. Based on Table 1, the final decision on the optimum parameters of the jet angle (α_1) and the blade angle (β_2) does not exist. Then, precision manufacturing technology for Turgo turbine blade manufacturing has not received special attention, whereas the Gaiser *et al.,* [11] PSTT blade fabricated using tablespoons. Therefore, this study aims to evaluate the α_1 and the geometry of the PSTT blade using velocity triangle analysis, then the design of the blade is manufactured using a three-dimensional (3D) printing machine for performance tests.

2. Method

2.1 Velocity Triangle Analysis

The design of PSTT using analytical methods starts by determining boundary conditions. Four boundary conditions are set: α_1 of 15° to 25°; β_1 of 40°; H of 3 m; Q of 0.26 lps. The analysis of geometry PSTT blade using Figure 1.

Based on the boundary conditions, determine the inlet section, i.e., the absolute water velocity (C_1), the relative water velocity (W_1), and runner rotational velocity (U).

$$C_1 = C_d\sqrt{2 \cdot g \cdot H} \tag{1}$$

where C_d is discharge coefficient of 0.91 [12]. U/C_{1x} is 0.5 to get the optimum PSTT performance; this condition is reach at $\beta_1 \sim 40°$. Advance determining U, C_1 is projected in the X-direction. Based on Figure 1, determine W_1 become

$$W_1 = \frac{C_{1r}}{\cos(90° - \beta_1)} \tag{2}$$

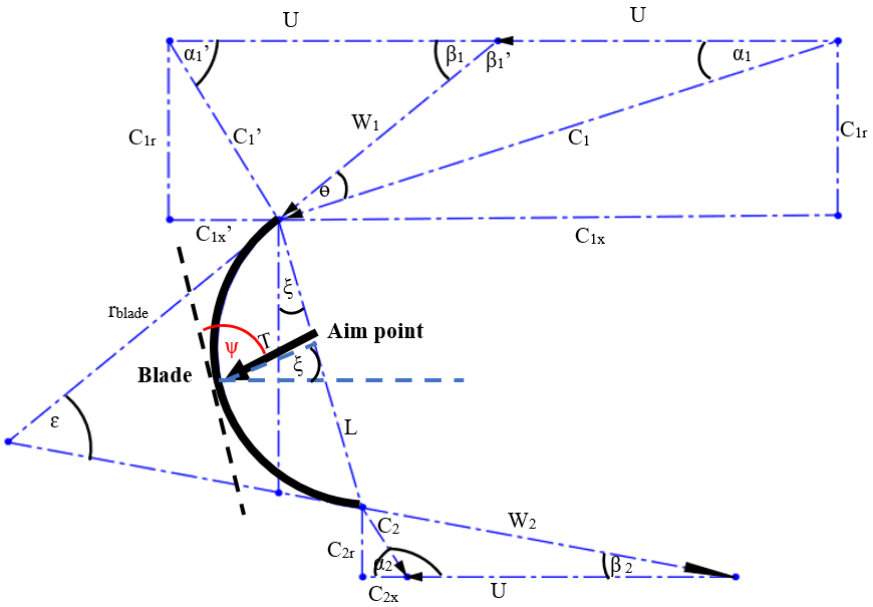

Fig. 1. Velocity triangle schematic on PSTT blade

In this case, the water passing through the blade wall is friction with the wall, so $W_2=W_1 \cdot 0.95$. The β_2 of 10°. Then, calculate the C_2 using the Pythagorean theorem, become

$$C_2 = \sqrt{U^2 + W_2^{\,2} - 2 \cdot U \cdot W_2 \cdot \cos\beta_2} \tag{3}$$

Based on Figure 1, the jet impact (C_1) to the blade split becomes two components: top ($\dot{m}_2$' and C_{2x}') and bottom ($\dot{m}_2$ and C_{2x}) [10]. The component to top is considered as losses; the mathematical analysis for $\dot{m}_2$' and C_{2x}'

$$\dot{m}_2{}' = Q \cdot \rho \cdot \sin^2\left(\frac{90 - \alpha_1 - \xi}{2}\right) \tag{4}$$

where ξ is a function of blade angle (ε) and β_2; ε is β_1 added β_2. The analysis mathematic for ξ

$$\xi = 90° - \left(\frac{180° - \varepsilon}{2}\right) - \beta_2 \tag{5}$$

Then, the C_{1x}' is analysed into ΔC_x'

$$\Delta C_x{}' = C_{1x} - C_{1x}{}' \tag{6}$$

C_{1x}' is the function of α_1' and C_1'. Based on Figure 1, α_1' and C_1' can be found using the Pythagorean theorem; C_1'is a function of W_1, U, and β_1; and α_1' is a function of U, C_1', and W_1. Further, the mathematical analysis of the bottom component becomes

$$\dot{m}_2 = Q \cdot \rho \cdot \cos^2\left(\frac{90 - \alpha_1 - \xi}{2}\right) \tag{7}$$

$$\Delta C_x = C_{1x} - C_{2x} \tag{8}$$

C_{1x} and C_{2x} is determined using the law of cosines. Therefore, the Euler approach for determining P_{mech} of PSTT becomes

$$P_{mech} = \left(\dot{m}_2 \cdot \Delta C_x + \dot{m}_2 ' \cdot \Delta C_x '\right) \cdot U \tag{9}$$

Then, PSTT performance is

$$\eta = \frac{P_{mech}}{\rho \cdot g \cdot Q \cdot H} \times 100\% \tag{10}$$

2.2 Runner Geometry Analysis

Diameter runner (D) is a function of U and angular velocity of runner (ω). The generator used is a direct current (DC) type with a specification of 250 rpm. Then, number of blade (z) is determine using Pelton turbine approach

$$z = 0.6 \cdot \sqrt{\frac{D}{d}} \tag{11}$$

d is jet diameter. Then, ratio of L/T of 0.5, and L/d of 2 to 6.

2.3 Experimental Setup

Figure 2 is an experimental setup for laboratory-scale PSTT testing. Installation of flow meter, elbows, and valves in Figure 2 on fully developed flow conditions; fully developed flow is predicted that occur in 32 diameters of pipe [13]. From Figure 1, the data obtained from the experiment are runner rotation (n) (rpm), voltage direct current (V), current (I), and flowrate or discharge (Q). Data n is obtained using the E18-D80NK sensor, V using the VCC 24V sensor, I using the ACS sensor, and Q using the YF-DN40 sensor. An 8-bit microcontroller is used as a data logger; 8-bit is considered capable of data acquisition for a PSTT test system [14]. There were 3 jet diameters (d) used in the test: 10 mm, 9 mm, and 8 mm. PSTT generated power calculation

$$P_{elec} = V \cdot I \tag{12}$$

The experimental setup materials in Figure 1 are: where 1 is the microcontroller, 2 is the pump, 3 is the water tank, 4 is the ACS sensor; 5 is the E18-D80NK sensor, 6 is the DC generator, 7 is the PSTT runner, 8 is a computer, 9 is the water tank, 10 is YF-DN40 sensor, 11 is the pipe, 12 is VCC 24V sensor.

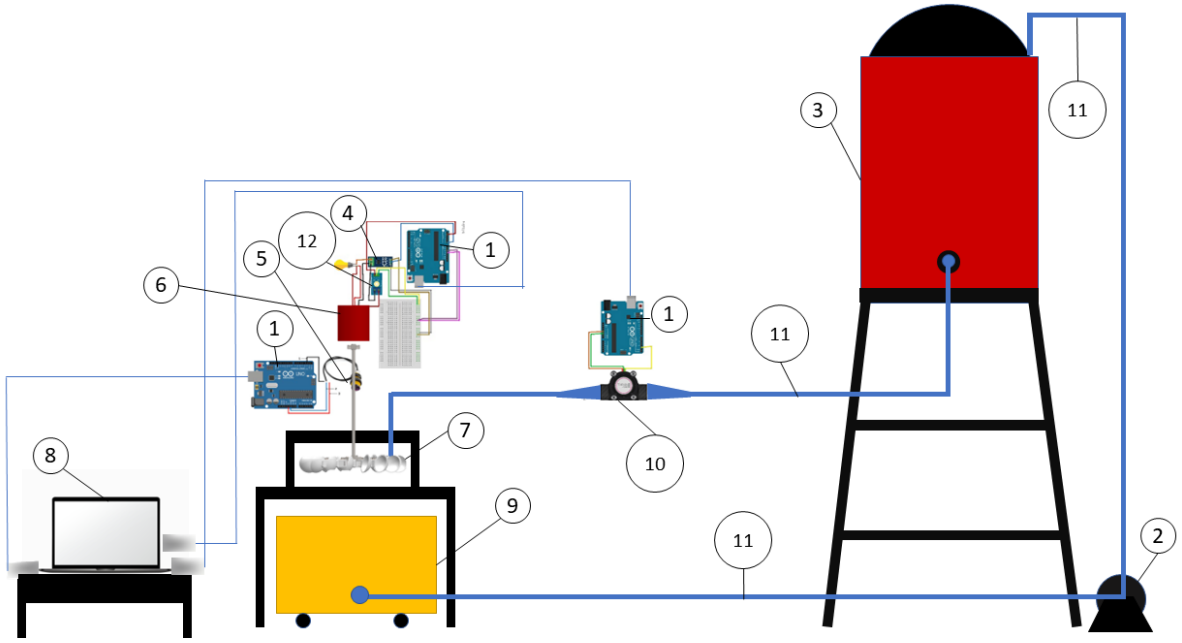

Fig. 2. Experimental Setup

Data generated by the four sensors were tested for uncertainty and error. The confidence level of the uncertainty test is 95%—uncertainty analysis following references [14,15]. For error analysis, the commercial measurement instruments are used as validator data. The four sensors with an 8-bit microcontroller system are considered useful because they have uncertainty below 2% (precision) and error below 10% (accurate). The results of uncertainty and error analysis are: tachometer uncertainty of 0.04% and error 0.5%; flowmeter uncertainty 0.87% and error -9.13%; multimeter for current uncertainty 1.37% and error 5.25%, and voltage uncertainty 0.01% and error 0.81%.

3. Results and Discussion

3.1 Analytical Results

PSTT blade design uses a velocity triangle to find the maximum and minimum specified boundary conditions. The PSTT blade model is based on the analytical results.

At the inlet, based on Eq. (1), C_1 of 6.98 m/s. Using trigonometry concepts, for 15° α_1, C_{1x} of 6.74 m/s and C_{1r} of 1.81 m/s, and for 25° α_1, C_{1x} of 6.33 m/s and C_{1r} of 2.95 m/s. Then, using Eq. (2), for 15° α_1, W_1 of 2.81 m/s and 25° α_1 of 4.59 m/s. Then, the calculation of U using Pythagorean concepts. Based on the calculation, α_1 increases U decreases and vice versa. For case 40° β_1, the magnitude of U equals W_1; the schematic velocity triangle at the inlet is isosceles.

At the outlet, W_2 is 95% of W_1. W_1 and W_2 are inversely related to U. Then, after U and W_2 are known, calculate C_2 using Eq. (3). Based on the calculations using Eq. (3), the magnitude of C_2 decreases on α_1 of 15° to 22° while on α_1 of 23° to 25°, it increases. Meanwhile, C_{2x} decreases from α_1 of 15° to 25° because of the vector of C_{2x} toward the inlet side.

Backflow to the inlet is considered a loss (Figure 1). Based on Figure 1, the magnitude (quantity) C_1' and $\dot{m}_2'$ is calculated using the momentum balance analysis [10]. Based on analysis using

momentum balance, C_1' is similar to C_2 where from α_1 of 15° to 22° it decreases and from 23° to 25° increases. Decreasing C_{1x}' because α_1' increased; α_1 of 15° to 22° is opposite to U and C_1 where these conditions mean that the backflow (C_1') and C_1 are one vector (inhibit). Table 2 summaries the results of calculations using the velocity triangle concept.

Table 2
PSTT velocity triangle calculation results

α_1 (°)	Inlet				Outlet			Losses		
	C_{1x} (m/s)	C_{1r} (m/s)	W_1 (m/s)	U/C_{1x} (m/s)	W_2 (m/s)	C_2 (m/s)	C_{2x} (m/s)	C_1' (m/s)	α_1' (°)	C_{X1}' (m/s)
15	6.74	1.81	2.81	0.68	2.67	2.01	1.96	3.03	36.56	2.44
16	6.71	1.92	2.99	0.66	2.84	1.69	1.62	2.87	42.17	2.12
17	6.68	2.04	3.18	0.64	3.02	1.38	1.27	2.73	48.42	1.81
18	6.64	2.16	3.36	0.61	3.19	1.08	0.93	2.63	55.23	1.50
19	6.60	2.27	3.54	0.59	3.36	0.83	0.58	2.56	62.49	1.18
20	6.56	2.39	3.71	0.57	3.53	0.66	0.24	2.54	70.00	0.87
21	6.52	2.50	3.89	0.54	3.70	0.65	-0.11	2.56	77.51	0.55
22	6.47	2.62	4.07	0.52	3.87	0.81	-0.45	2.63	84.77	0.24
23	6.43	2.73	4.24	0.49	4.03	1.06	-0.79	2.73	91.58	-0.08
24	6.38	2.84	4.42	0.47	4.20	1.35	-1.14	2.87	97.83	-0.39
25	6.33	2.95	4.59	0.44	4.36	1.67	-1.48	3.03	103.44	-0.71

Figure 3 shows the calculation results of Eq. (4) to Eq. (10) using the data in Table 2. Figure 3(a) is the relation of $\dot{m}_2$, $\dot{m}_2'$, ΔC_x, and $\Delta C_x'$ to α_1. Based on calculations Eq. (4) to Eq. (8), α_1 increases $\dot{m}_2$, ΔC_x, and $\Delta C_x'$ increased while $\dot{m}_2'$ decreased. The decrease in $\dot{m}_2'$ is because of ψ decrease (the law of mass and momentum balance). Eq. (4) to Eq. (8) is verified because the 15° α_1 is aimed at point 90° against the blade wall (Figure 1); therefore, $\dot{m}_2$ equal $\dot{m}_2'$. Figure 3(b) is the relation of P_{mech} and η to α_1. Based on calculations Eq. (9) and Eq. (10), the peak performance is 20° α_1. The maximum PSTT performance is predicted to occur at 20° α_1, similar to Williamson *et al.,* [10] and Cobb [16]; this indicates that the mathematical analysis is verified.

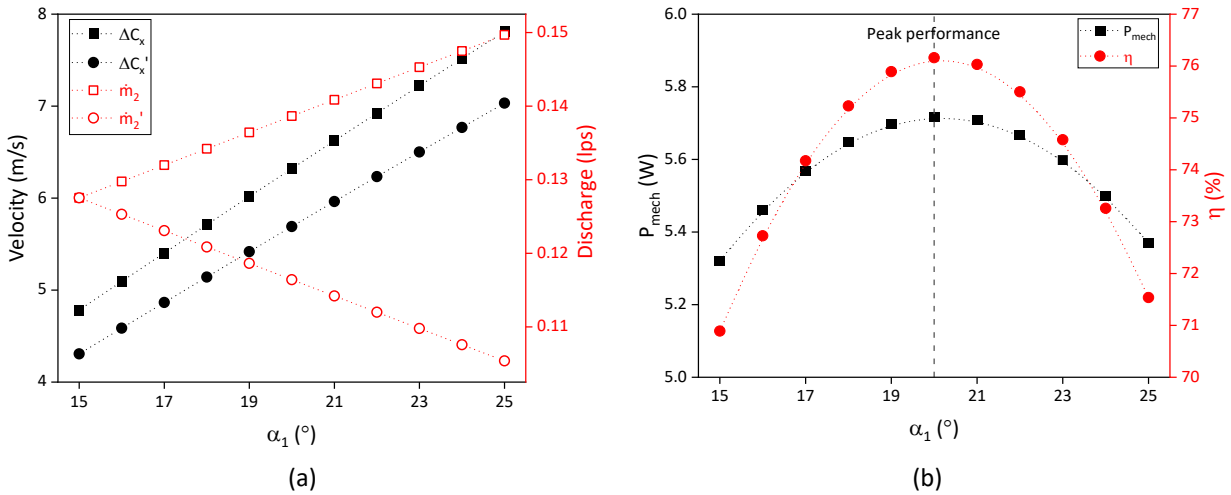

Fig. 3. Analytical results: (a) Relation of $\dot{m}_2$, $\dot{m}_2'$, ΔC_x, and $\Delta C_x'$ to α_1; (b) Relation of P_{mech} and η to α_1

Based on Figure 3, U/C_{x1} for ° α_1 of 0.57; means U of 3.71 m/s. Specification DC generator of 250 rpm so that ω of 27 rad/s; therefore, D of 0.275 m (275 mm). Further, using Eq. (11), z of 16.5 due to manufacturing considerations, z is rounded down. Then, L of 5.8 cm and T of 2.9 cm. Figure 4 shows the shape of the PSTT blade and runner due to the design.

(a) (b)

Fig. 4. PSTT runner: (a) Blade manufacturing process using three-dimensional printing machine; (b) Runner design

3.2 Experimental Results

3.2.1 Relationship P_{pot} to V_{jet}

Based on Eq. (10), the potential energy of water (P_{pot}) is a function of the jet velocity (V_{jet}). Figure 5 shows the relation of V_{jet} to P_{pot} is exponential. Based on Figure 5, P_{pot} maximum apparatus setup of 9.02 W with V_{jet} of 4.04m/s and d of 10 mm, and P_{pot} minimum of 4.45 W with V_{jet} of 3.11 m/s and d of 8 mm.

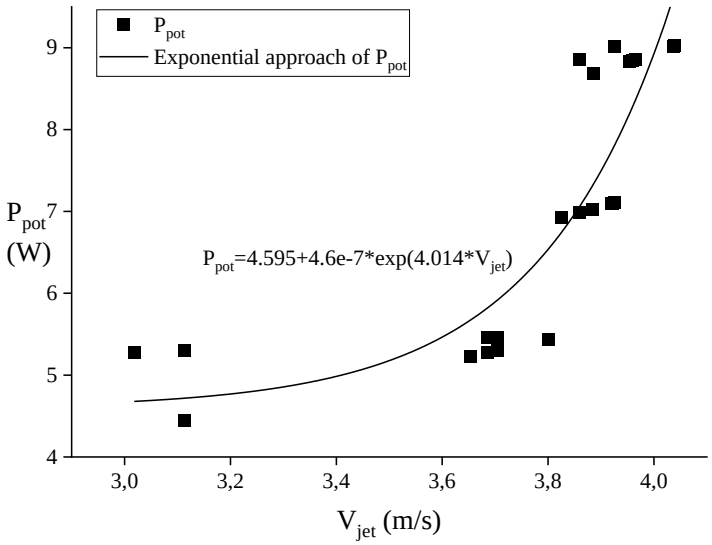

Fig. 5. Relation of Vjet to Ppot

3.2.2 Relationship V and I to n

The lamp was used as a load. There are three variations of the loads: 3 W, 5 W, and 10 W. Figure 6 is the test results. Figure 6(a) is the relation of V to n. Based on Figure 6(a), 3 W load test results show PSTT produces the highest V of 8.31 V_{dc} at 243.43 rpm. For a 5 W load, the highest V is 9.82 V_{dc} at 220.66 rpm. And for the 10 W load, the highest V is 8.87 V_{dc} at 241.63 rpm. Based on Figure 6(a), the highest V is produced using a 5 W load.

Figure 6(b) is the relation of I to n; increasing n increases I. Based on Figure 6(b), the minimum I generated by the PSTT is 20.62 mA at n of 194.54 rpm (3 W load and 8 mm nozzle). The peak I generated is 182.49 mA at n of 245 rpm (3 W load and 10 nozzles).

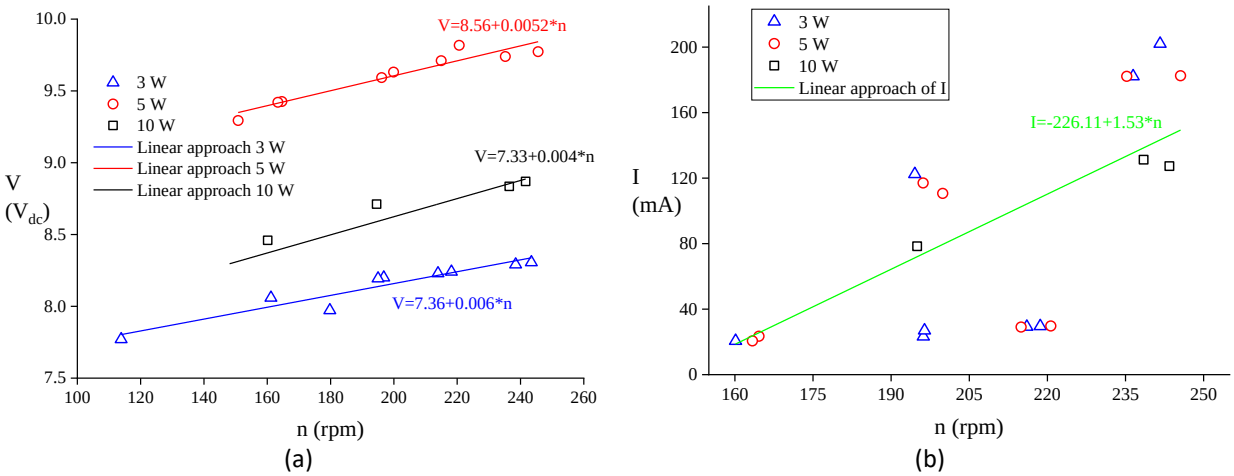

Fig. 6. Experimental results: (a) Relation of V to n; (b) Relationship I to n

3.2.3 Relationship P_{gen} to n

Figure 7 is the relation of P_{gen} to n. Based on Figure 7, the use of 3 W and 5 W loads produces a different power from the use of 10 W load; the 3 W and 5 W loads show a significant increase in power than of 10 W. Based on Figure 7, P_{gen} peak produced by PSTT for 3 W load is 1.79 W at 241.64 rpm, 5 W load is 1.78 W at 245.57 rpm, and 10 W load is 1.09 W at 238.48 rpm. Whereas P_{gen} minimum produced for 3 W load is 0.17 W at 160.14 rpm, 5 W load is 0.19 W at 163.37 rpm, and 10 W load is 0.49 W at 163.37 rpm.

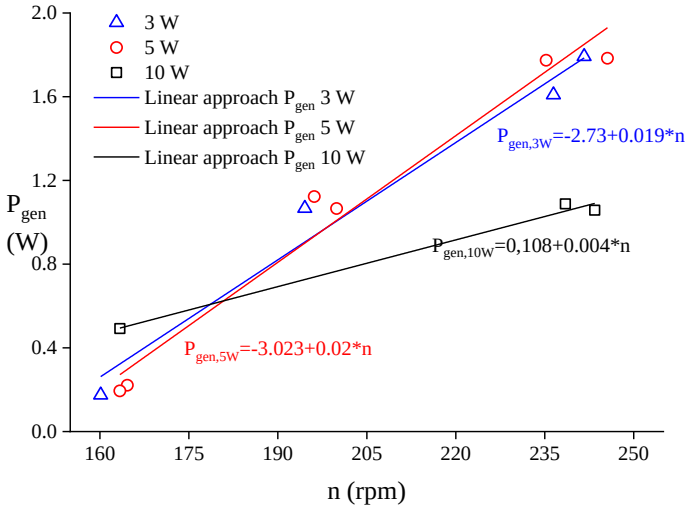

Fig. 7. Relation of P_{gen} to n

3.2.4 Relationship η to n

Figure 8 shows the relation of η to n; the relation is polynomial cubic. Based on Figure 8, the PSTT peak performance is 25.44% with a load of 5 W and 150.81 rpm, and the lowest of 9.01% with a load of 10 W and 113.99 rpm. Then, PSTT stable performance is 19.97%, with an operating range of 190 rpm to 240 rpm. The PSTT peak working condition is 164.5 rpm based on the polynomial cubic approach. The decrease in performance occurs at a load of 10 W, which is allegedly due to the high load, so the system requires ample torque. The large torque makes the turbine rotation decrease. The decrease in turbine rotation is a disadvantage for the system. Because the minimum rotation generator produces voltage is not achieved. Figure 9 is a laboratory-scale PSTT test documentation.

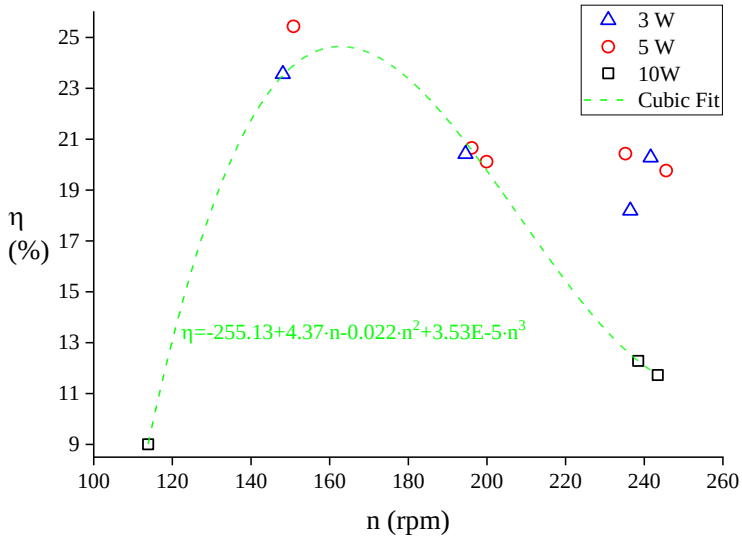

Fig. 8. Relation of η to n

PSTT blades in Figure 9 is manufacture using 3D printing. Due to massive technology developments, manufacture of PSTT blade is cheaper and easier than utilizing of spoon of coconut shell and stainless steel [17,18]. Since the coconut sheel before being used as a spoon requires special treatment such as sandpaper, size adjustment, dying, and painting. Then, the stainless steel spoon assembly to the wheel is welded where welding technology is rare in remote areas and requires a large of electrical energy.

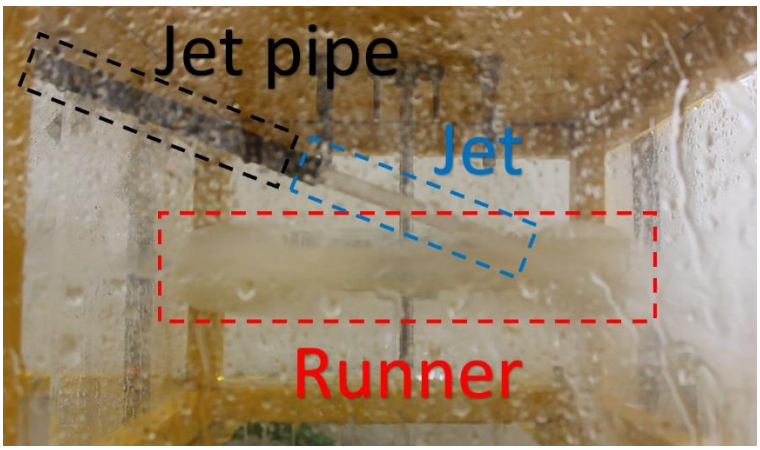

Fig. 9. PSTT testing

3.3 Comparison of Experimental Results to Analytical Data

Table 3 compares experimental results with the velocity triangle analysis approach; the comparison variable is d of 8 mm and 10 mm. From Table 3, the average deviation of analytics to experimental is 6.6%. Therefore, mathematical analytics using a velocity triangle approach for PSTT blade and runner design is recommended to be implemented.

Table 3
Comparison of experimental results to analytical data

d	P_{gen} (W)		η (%)		Deviation
(mm)	Exp.	Ana.	Exp.	Ana.	(%)
8	1.02	1.54	25.43	24.08	5.61
10	1.78	2.21	23.55	25.48	7.58
Average					6.6

4. Conclusions

The global warming issue drives pico-scale hydropower plants to become the leading research focus. PSTT is a suitable proposal to be developed as a power plant because it is cheap, easy to manufacture, and simple in shape and design [10]. Although it has been developed for a long time, there is no standard empirical equation in designing the PSTT. Therefore, this study aims to review the feasibility of the velocity triangle approach as an empirical equation for designing PSTT. Then, the velocity triangle approach is used to evaluate the appropriate the α1 for PSTT because there is no final decision yet. Based on comparing experimental results to analytical data, the velocity triangle approach is recommended for designing PSTT because of the average deviation of 6.6% (deviation is reasonable). Further, based on calculations results, the peak PSTT performance is predicted to occur at 20° α_1, where this hypothesis is similar to Williamson *et al.,* [10] and Cobb's [16] study; this indicates that the mathematical analysis is verified.

Furthermore, from the experiment results, printing PSTT blades using a 3D printing machine is recommended because of the ease in the manufacturing process, the time required in the manufacturing process is not long, and the low cost becomes the principal value in recommending 3D printing machines.

Acknowledgement
The research/publication of this article was funded by DIPA of Public Service Agency of Universitas Sriwijaya 2022. SP DIPA-023.17.2.677515/2022, on December 13, 2021. In accordance with Dean's Decree Number: 1440/UN.9.FKIP/TU.SK/2022.

References
[1] Siswantara, Ahmad Indra, Budiarso Budiarso, Aji Putro Prakoso, Gun Gun R. Gunadi, Warjito Warjito, and Dendy Adanta. "Assessment of turbulence model for cross-flow pico hydro turbine numerical simulation." *CFD Letters* 10, no. 2 (2018): 38-48.

[2] Williamson, Sam J., Bernard H. Stark, and Julian D. Booker. "Low head pico hydro turbine selection using a multi-criteria analysis." *Renewable Energy* 61 (2014): 43-50. https://doi.org/10.1016/j.renene.2012.06.020

[3] Warjito, Budiarso, A. I. Siswantoro, Dendy Adanta, M. Kamal, and R. Dianofitra. "Simple bucket curvature for designing a low-head Turgo turbine for pico hydro application." *International Journal of Technology* 8, no. 7 (2017): 1239-1247. https://doi.org/10.14716/ijtech.v8i7.767

[4] Adanta, Dendy, Imam Syofii, Dewi Puspita Sari, and Apri Wiyono. "Performance of Pico Scale Turgo Turbine in Difference the Nozzle Diameter." *International Journal of Fluid Machinery and Systems* 15, no. 1 (2022): 130-136. https://doi.org/10.5293/IJFMS.2022.15.1.130

[5] Khattak, M. A., N. S. Mohd Ali, N. H. Zainal Abidin, N. S. Azhar, and M. H. Omar. "Common Type of Turbines in Power Plant: A Review." *Journal of Advanced Research in Applied Sciences and Engineering Technology* 3, no. 1 (2016): 77-100.
[6] Atmoko, M. Hari. "Tim Ekspedisi Papua Terang Rekomendasikan Penggunaan Piko Hidro." *ANTARA News*. October 16 2019.
[7] Budiarso, Budiarso, Warjito Warjito, and Dendy Adanta, "Kajian Turbin Air Piko Hidro Daerah Terpencil Di Indonesia." in *Proceeding Seminar Nasional Tahunan Teknik Mesin XV*, p. 301-307. Bandung, 2016.
[8] Benzon, D. S., George Athanasios Aggidis, and J. S. Anagnostopoulos. "Development of the Turgo Impulse turbine: Past and present." *Applied Energy* 166 (2016): 1-18. https://doi.org/10.1016/j.apenergy.2015.12.091
[9] Sakulphan, Kiattisak, and Erik L. J. Bohez. "A new optimal selection method with seasonal flow and irrigation variability for hydro turbine type and size." *Energies* 11, no. 11 (2018): 3212. https://doi.org/10.3390/en11113212
[10] Williamson, Sam J., Bernard H. Stark, and Julian D. Booker. "Performance of a low-head pico-hydro Turgo turbine." *Applied Energy* 102 (2013): 1114-1126. https://doi.org/10.1016/j.apenergy.2012.06.029
[11] Gaiser, Kyle, Paul Erickson, Pieter Stroeve, and Jean-Pierre Delplanque. "An experimental investigation of design parameters for pico-hydro Turgo turbines using a response surface methodology." *Renewable Energy* 85 (2016): 406-418. https://doi.org/10.1016/j.renene.2015.06.049
[12] Židonis, Audrius, David S. Benzon, and George A. Aggidis. "Development of hydro impulse turbines and new opportunities." *Renewable and Sustainable Energy Reviews* 51 (2015): 1624-1635. https://doi.org/10.1016/j.rser.2015.07.007
[13] Munson, Bruce R., Donald F. Young, and Theodore H. Okiishi. *Fundamentals of fluid mechanics*. 5th Ed. Wiley, 2006.
[14] Adanta, Dendy, and Dwijaya Febriansyah. "Simple micro controller measurement devices for pico hydro turbines." *International Review of Mechanical Engineering* 13, no. 8 (2019): 471-480. https://doi.org/10.15866/ireme.v13i8.17453
[15] Coleman, Hugh W., and W. Glenn Steele. *Experimentation and Uncertainty Analysis for Engineers*. 2nd Ed. Wiley-Interscience, 1999.
[16] Cobb, Bryan R. "Experimental study of impulse turbines and permanent magnet alternators for pico-hydropower generation." *PhD diss., Oregon State University*, 2011.
[17] Adanta, Dendy, Warjito Warjito, Dwijaya Febriansyah, and Budiarso Budiarso. "Feasibility analysis of a pico-scale turgo turbine bucket using coconut shell spoons for electricity generation in remote areas in Indonesia." *Journal of Advanced Research in Fluid Mechanics and Thermal Sciences* 69, no. 1 (2020): 85-97. https://doi.org/10.37934/arfmts.69.1.8597
[18] Budiarso, Budiarso, Warjito Warjito, M. Naufal Lubis, and Dendy Adanta. "Performance of a low cost spoon-based turgo turbine for pico hydro installation." *Energy Procedia* 156 (2019): 447-451. https://doi.org/10.1016/j.egypro.2018.11.087